

# HR Diagrams and Clustering Analysis of Open Cluster M6 and Globular Cluster M13

June 2023

## Contents

<b>I</b>	<b>Introduction</b>	<b>2</b>
A	Our Clusters . . . . .	2
A.1	M13 . . . . .	2
A.2	M6 . . . . .	2
<b>II</b>	<b>Background and Importance</b>	<b>2</b>
A	Hertzsprung-Russell Diagrams . . . . .	2
B	Globular Clusters . . . . .	3
C	Open Clusters . . . . .	3
D	Larger Context . . . . .	4
<b>III</b>	<b>Data Collection</b>	<b>4</b>
A	Image Requests . . . . .	4
B	Aligning . . . . .	5
<b>IV</b>	<b>Data</b>	<b>7</b>
A	Image Analysis . . . . .	7
A.1	Identifying Sources . . . . .	7
A.2	Masking and Filtration . . . . .	7
B	Aperture Photometry . . . . .	8
C	Initial HR Diagrams . . . . .	9
D	Sigma Clip . . . . .	9
E	Reference Stars . . . . .	10
F	Final HR Diagrams . . . . .	13
<b>V</b>	<b>Final Analysis</b>	<b>14</b>
A	M13 . . . . .	14
B	M6 . . . . .	14
C	M13 & M6 . . . . .	14
<b>VI</b>	<b>Error Analysis</b>	<b>15</b>
A	Signal to Noise Ratio . . . . .	15
B	Linear Fit . . . . .	16
<b>VII</b>	<b>Conclusion</b>	<b>17</b>
	<b>Appendices</b>	<b>20</b>

# I Introduction

Star clusters are collections of stars that are held together by self-gravitation. They can range in size, shape, and age, but there are two main categories, open clusters and globular clusters. One way that astronomers analyze star clusters is by creating Hertzsprung-Russell (HR) diagrams which depict the relationship between the apparent magnitudes and temperatures of the stars in the cluster. Using CCD camera images, we made our own HR diagrams of the globular cluster M13 and the open cluster M6. We analyzed what the diagrams reveal about these individual clusters and used them to compare the different types of clusters.

## A Our Clusters

### A.1 M13

M13 is a globular star cluster containing several hundred thousand stars. It is located in the constellation Hercules and is one of the best-known clusters in the Northern Hemisphere. Its integrated apparent magnitude is 5.8, and its brightest star, V11, is a variable red giant of magnitude 11.95. M13 is estimated to be 11.66 billion years old and 6.8 kpc away from Earth [8].



Figure 1: Color image of M13. Credit: Sid Leach at Mount Lemmon SkyCenter [5]



Figure 2: Color image of M6 Credit: Giuseppe Donatiello [1]

### A.2 M6

M6, also known as the Butterfly Cluster due to its stars forming a shape vaguely resembling a butterfly, is an open cluster in the constellation Scorpius. It has an estimated 120 stars, much fewer than M13. Its integrated magnitude, however, is brighter than M13 at 4.2, and its brightest star BM Scorpi, a K-type orange giant star, has a variable magnitude ranging from 5.5 to 7. M6 is much younger than M13, only 94.2 million years old. Astronomers estimate it to be 0.487 kpc away from Earth [7].

# II Background and Importance

## A Hertzsprung-Russell Diagrams

HR diagrams, also known as color-magnitude diagrams when pertaining to star clusters, plot the temperature of stars against their magnitudes. First developed in the early 1910s by Ejnar Hertzsprung and Henry Norris Russell, HR diagrams have been key tools in the study of stellar evolution.

Diagrams like the one depicted in figure 3 plot absolute magnitude vs spectral type. These plots are not for a single cluster, but for a collection of known stars without a common distance or location in the sky. However, when making an HR diagram for a star cluster, plotting the apparent magnitudes instead of absolute magnitudes does not change any trends on the graph. Since apparent magnitude is related to absolute magnitude solely by distance, and all of the stars in a cluster are around the same distance from Earth, a plot of absolute magnitudes would just be a translation of a plot of apparent magnitudes and the shape would be preserved.

The trends on these scatter plots can display information about the characteristics of the included stars. Most stars, including our sun, fall in the main sequence region of the graph, the large diagonal strip in figure 3. Main sequence stars are in a relatively early stage in their life in which they fuse hydrogen in their cores. Other regions of the diagram include giants in the top right and dwarves in the bottom left. Stars in these sections are in later stages of life than main sequence stars. This categorization allows astronomers to dissect a star's life cycle and relate the stages to trends in temperature and luminosity [3].

## B Globular Clusters

Globular clusters, like our target M13, are stable, tightly bound collections of stars. They contain anywhere from tens of thousands to millions of stars and can be found in any type of galaxy. They tend to contain older, and therefore, redder stars. They contain little free dust and gas, so they are not an environment suited for new star formation. Due to their concentrated centers, they can be a more challenging subject for astronomers as the stars in the middle are less distinct [2].

## C Open Clusters

Open clusters, like our target M6, are more loosely bound. They contain fewer stars, on the order of ten to a few hundred. Open clusters are limited to spiral and irregular or spiral galaxies and are sometimes referred to as galactic clusters due to their prominence in the dusty arms of spiral galaxies. Stars in these clusters are also of a wider range of ages and temperatures. Their less dense nature makes observing individual stars much easier [9].

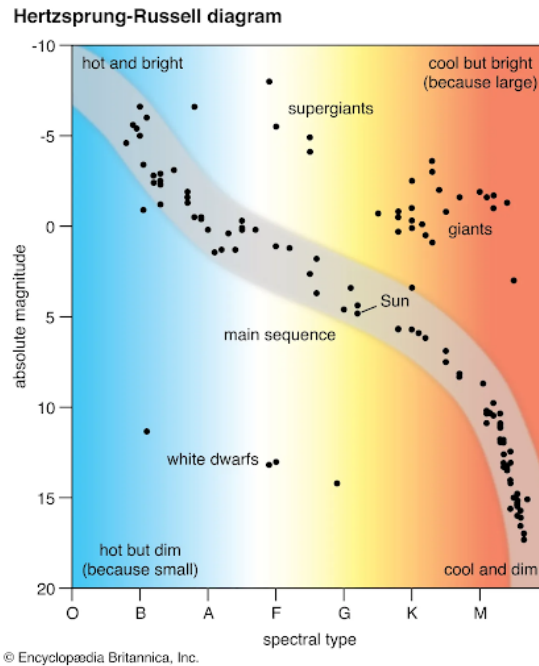


Figure 3: Simulated HR diagram that shows general structure of such diagrams. Credit: Encyclopædia Britannica.

## D Larger Context

HR diagrams of clusters can, first, be used to organize stars based on their individual locations on the plot. We can point at any star on the diagram and immediately determine its spectral class and apparent magnitude.

Taking a step back, we can examine, more qualitatively, the shape that the stars make together on the graph. We can identify what portion of the stars in the cluster are main sequence, red giants, white dwarfs, etc. The color at which the stars tend to become red giants is known as the turnoff point. Determining the turnoff point for a cluster is a clue in calculating the age of a cluster as redder turnoff points correspond to older clusters.

Beyond that, we can compare our two HR diagrams. This can provide insight into the similarities and differences between open clusters and globular clusters. Comparing the turnoff points for M6 and M13, we can confirm (or deny) that globular clusters are older and redder than open clusters.

## III Data Collection

Our first task in this investigation was to choose our observation targets. We had the privilege of having access to the LCO global telescope network, affording us the ability to view a wide range of targets at any declination. We were restricted to a certain range of right ascensions, as that visibility depends on the time of year, not location on the earth. We were also limited to objects of a certain magnitude, hoping to find targets between magnitudes 4 and 15. After narrowing our search, interested in finding one globular cluster and one open cluster, we landed on M13 and M6. M6 was viewable nearly at the zenith from three locations, and M13 had a maximum altitude of over  $80^\circ$  from three locations as well [A3].

To make HR diagrams, we needed CCD (Charge-Coupled Device) images of our clusters in different filters. CCD cameras detect incoming photons and convert them into electrons for a digital flux output. Using filters, we can control the wavelength of the incoming light and only collect what we need. HR diagrams require a magnitude and temperature, which is analogous to color, for each star. The magnitude of a star can be taken directly from the flux output of the CCD camera. We chose to use the G band to find our apparent magnitude. Color cannot be found using just one filter. We needed a color index, which is a subtraction of the magnitudes in two filters, where the lower the color index, the bluer the object. We decided to do a G-R color index [6].

## A Image Requests

This approach meant that we needed images in the G band and R band for each object. For the sake of completeness, we decided to request images in I band and U band in addition to G and R. That way we could assess the images in all of the filters and confirm that we wanted to use G and R [A2].

We had access to LCO's SBIG 6303 0.4m telescope and decided to use the SDSS (Sloan Digital Sky Survey) filters. We requested the images listed in table 1. We requested multiple different exposure times to ensure that if any turned out to be under or oversaturated, we would have other images to choose from.

After comparing the images from different exposure times, we believed that the 10s exposure time returned the clearest images for both objects.

Target	RA	Dec	Filter	# Exposures	Integration Time
M13	17h 40m 16.6s	-32° 14' 31"	SDSS I	10	1, 10, 100
			SDSS R	10	1, 10, 100
			SDSS G	10	1, 10, 100
			SDSS U	10	1, 10, 100
M6	6h 41m 41s	+36° 27' 35"	SDSS I	10	10, 100
			SDSS R	10	10, 100
			SDSS G	10	10, 100
			SDSS U	10	10, 100

Table 1: Images we requested from LCO.

## B Aligning

We had ten images in each filter taken in 10s exposures. We first looked at each image to confirm that they had no irregularities, such as streaking, satellite traces, or noisy readouts. To maintain image quality, we aligned all ten images for each filter using the average function in Astroart 8. This ensures that signal outliers are averaged out. The aligned G and R images for each cluster are shown in figures 4 and 5. We used these aligned images for all further analyses.



(a) SDSS R 10x10s exposures averaged and aligned.



(b) SDSS R 10x10s exposures averaged and aligned.

Figure 4: M13 aligned CCD images.



(a) SDSS R 10x10s exposures averaged and aligned.



(b) SDSS R 10x10s exposures averaged and aligned.

Figure 5: M6 aligned CCD images.

Since we had all of the filters, we also used the trichromy function in Astroart to make an IRG color image of each of the clusters (figures 6 and 7). We can use these images later to compare with the color results of our HR diagrams. For instance, if an HR diagram suggests a heavily blue cluster, its color image should reflect that blue dominance as well.



Figure 6: IRG trichromy color image of M13.



Figure 7: IRG trichromy color image of M6.



## IV Data

### A Image Analysis

Now that we had all of our images, we could start using them to calculate the magnitudes and color indices of the stars in our clusters. We needed to translate the CCD flux output array into instrumental magnitudes that we could work with [A1].

#### A.1 Identifying Sources

First, we needed to identify the points in our images that actually represented stars. We tried a couple of different methods and functions for source identification [A4]. We landed on the Source Extractor algorithms from SEP (Source Extraction and Photometry), as it was best at distinguishing the stars in the center globular cluster and did not miss obvious stars in the open cluster. The SEP background function computes the representation of spatially variable image background and noise instead of averaging over pixels like other identification methods. This was effective in eliminating noise and irrelevant signals. The sources that SEP found in the G band for each filter are depicted in figures 8 and 9. Although the Source Extractor failed to find a few stars in each image and could not resolve the center of M13, there were plenty of sources to use in our diagrams.

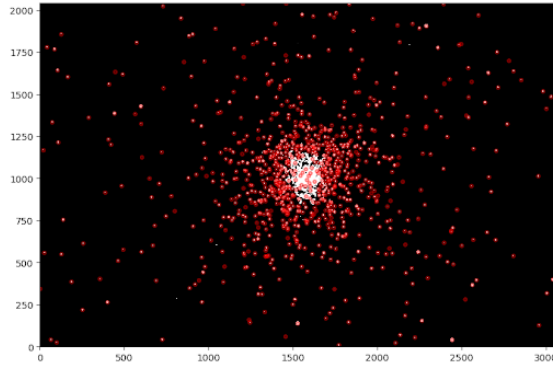


Figure 8: SEP identified sources in M13.

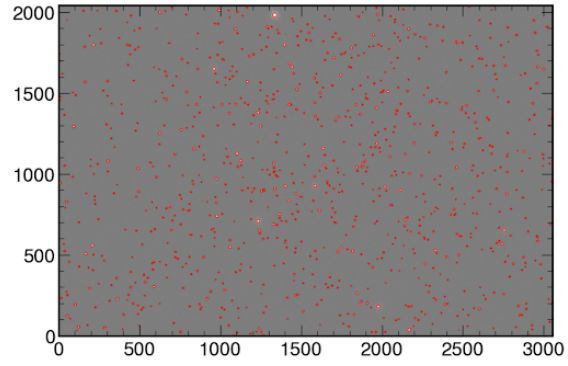


Figure 9: SEP identified sources in M6.

#### A.2 Masking and Filtration

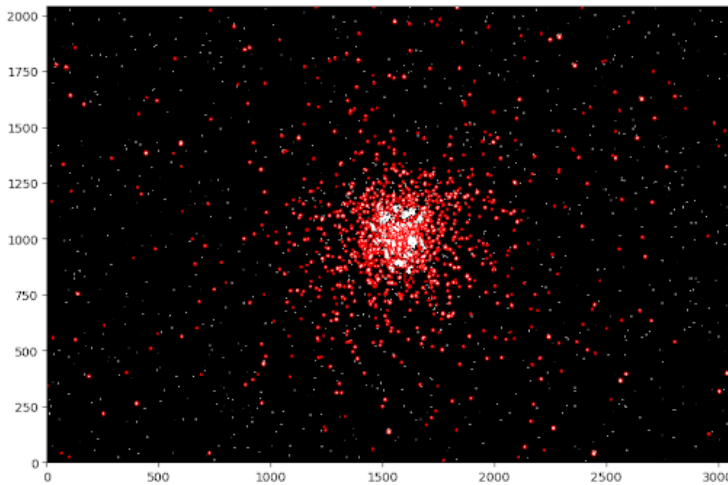


Figure 10: Sources in M13 with elliptical apertures.

We needed to manage the concerning low resolution in the center of M13. We plotted elliptical apertures around the SEP sources. This is shown to the left in figure 10. We only wanted to use circular sources, so we deleted sources that had a semi-major axis much longer than its semi-minor-axis. This removed the sources from the center of M13, depicted in figure 11, and left a more than sufficient amount of stars for our HR diagram.

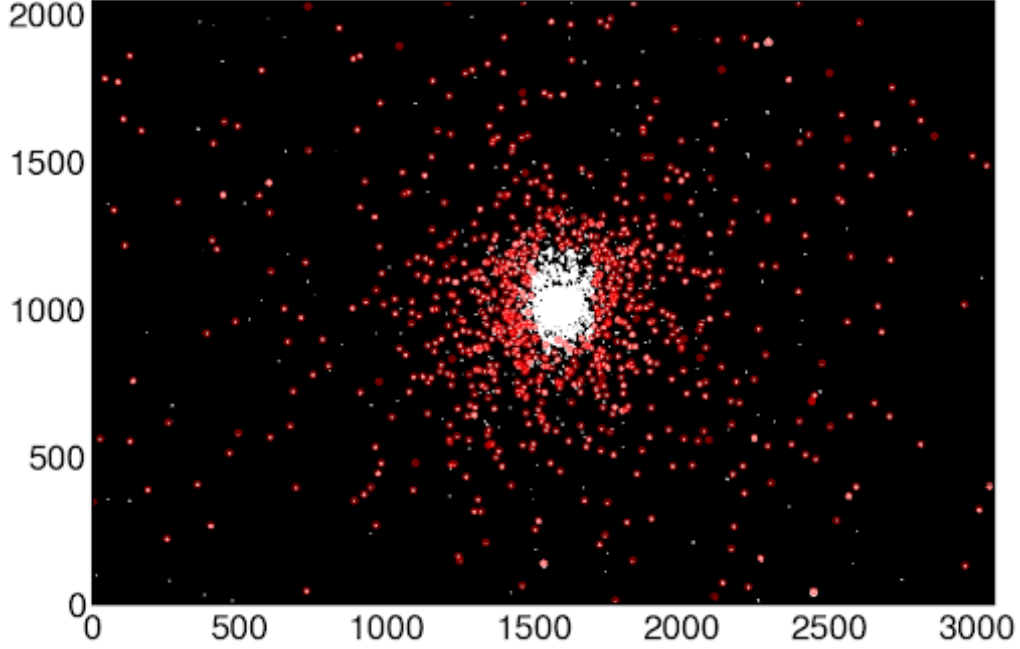


Figure 11: Masked sources for M13.

Since M6 is an open cluster, it did not need this sort of masking, but there were still sources that needed to be removed from both clusters. We needed to ensure that there were no sources picked up in one filter and not the other. We achieved this by neglecting sources that had very negative G-R fluxes. Having some amounts of subtracted fluxes below zero was to be expected as some sources are redder than they are green, but if G-R returned any fluxes that were too negative to be from color differences, those stars were omitted.

## B Aperture Photometry

Now that we had identified the sources we wanted to use in each cluster, the final step was to convert the fluxes provided by the CCD camera into instrumental magnitudes. Instrumental magnitudes are relative magnitudes, and they have no meaning outside of the cluster. Later on, we converted these instrumental magnitudes into usable apparent magnitudes, but instrumental magnitudes were adequate for preliminary analysis within the cluster.

We first had to estimate the center of the star point spread function. Then, implementing a 5 pixel aperture radius, we used the *aperture photometry* function in photutils on our background-subtracted images to sum the fluxes in our aperture for every source. Now that we knew the total flux of each star, we used the relations

$$M_{inst,G} = -2.5 \log(G_{sum}) \quad (1)$$

and

$$M_{inst,R} = -2.5 \log(R_{sum}) \quad (2)$$

to convert these fluxes into instrumental magnitudes. This process was completed for the R and G aligned images for both clusters.

We plotted the R instrumental magnitude against the G instrumental magnitudes for M13 and M6 to get a first look at what the color indices will be. They are shown in figures 12 and 13. From these plots, we can predict that M13 will be redder than M6 since the R magnitude values tend to be closer to the G magnitude values in the M13 plot.



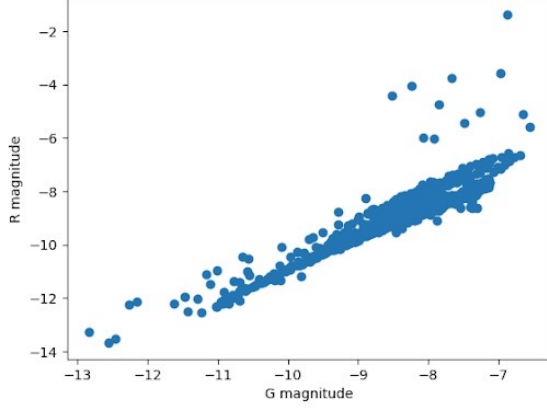


Figure 12: Plot of  $R_{mag}$  vs  $G_{mag}$  for M13.

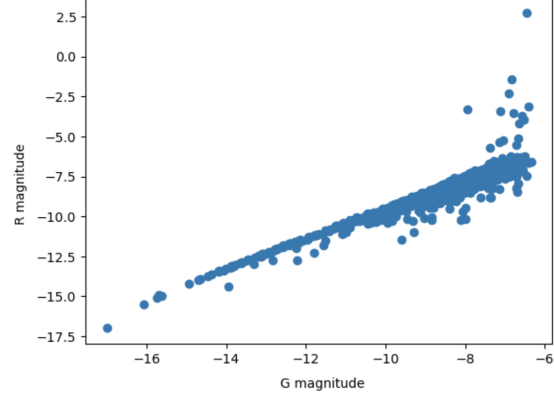


Figure 13: Plot of  $R_{mag}$  vs  $G_{mag}$  for M6.

## C Initial HR Diagrams

Once we had the G and R instrumental magnitudes for all of the sources, we had enough data to make our first HR diagrams. Depicted in figures 14 and 15, these raw, uncalibrated diagrams plot G instrumental magnitude against the difference in magnitudes G-R. These diagrams do not tell us anything quantitative about our clusters as the values on the axes are arbitrary. The shapes that the stars make in the diagrams, though, are the same shapes that will be in all of our HR diagrams; it is only translations and trimming from here.

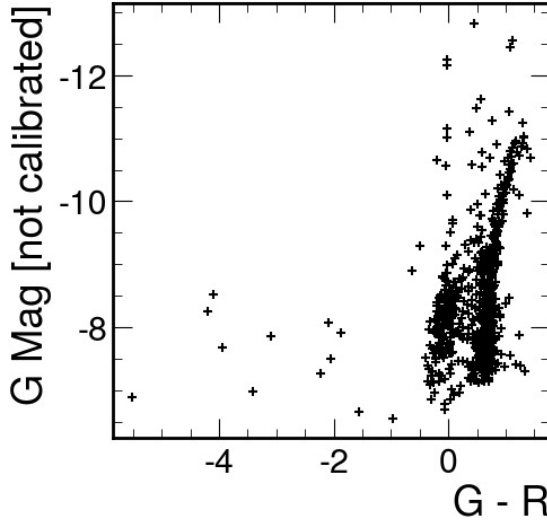


Figure 14: Raw, uncalibrated HR diagram of instrumental magnitudes for M13.

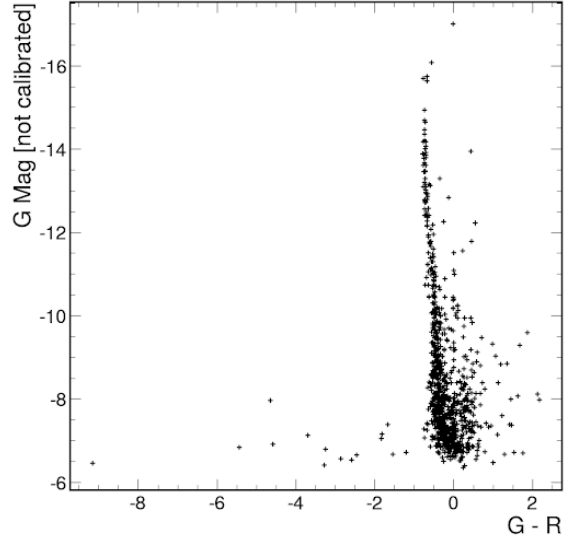


Figure 15: Raw, uncalibrated HR diagram of instrumental magnitudes for M6.

## D Sigma Clip

One challenge in creating our complete HR diagram was discerning which sources actually belonged to our star cluster. Not all unwanted signals are due to noise. When viewing objects that are thousands of light years away, there are bound to be other objects in front of and behind it that can appear in our field of view. One way to deduce which stars are in the cluster is to analyze the proper motions of the sources, as the stars in a cluster will move as a group, while the extraneous objects will have motion unrelated to the cluster. Alas, due to time and resource constraints, we

did not analyze proper motion. We did, however, use our personal judgment, coupled with previous works and statistical analysis, to decide which stars we believed were in our star clusters.

Figures 16 and 17 are the accepted HR diagrams that we referenced when choosing how to truncate our data. When comparing these plots to our uncalibrated HR diagrams in figures, we could see some resemblance in the concentrated regions of our diagrams, but knew we needed to cut out some outliers. We decided to implement a sigma clip of the data, which rejects values higher or lower than a certain number of standard deviations  $\sigma$  from the mean.

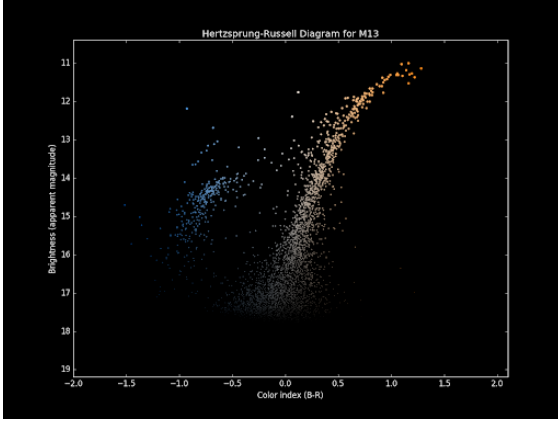


Figure 16: Accepted HR diagram of M13 that we used as a reference. Credit: Vleeming, G. [10]

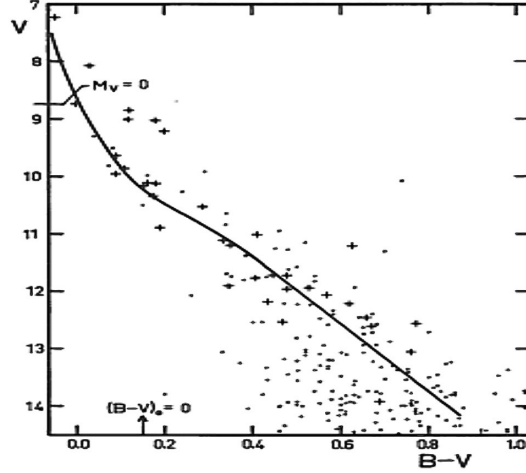


Figure 17: Accepted HR diagram of M13 that we used as a reference. Credit: Vanderbei, Bob [11]

After comparing the clipped data for different numbers of  $\sigma$  s with the accepted HR diagrams, we decided to use a  $3\sigma$  sigma clip on M13 and a  $1\sigma$  sigma clip on M6.

## E Reference Stars

If we were only curious about the shape of the HR diagram, we could have stopped work here. However, we wanted to convert these instrumental magnitudes into meaningful quantities. To do this, we needed to use reference stars. Reference stars are stars in our cluster with known apparent magnitudes that we can match with stars in our images to deduce the relationship between our calculated magnitudes and ones that are actually useful. Since all of the stars in a cluster are nearly the same distance from Earth, we can convert our instrumental magnitudes to apparent magnitudes by just adding a constant zero point such that,

$$M_{app} = M_{inst} + ZP. \quad (3)$$

To find ZP, we chose five reference stars in each cluster. Using the Star Atlas tool in Astroart, we were able to match the reference stars from our images to a database and get their apparent magnitudes from there. Figures 18 and 19 show this process.

Next, we had to find which instrumental magnitudes we calculated belonged to our five chosen stars. The database provided the Right Ascensions and Declinations of our reference stars, so we used the WCS *skycoord to pixel* function to convert those given coordinates into pixel values that we could employ in our images. After inputting the sky coordinates, we confirmed that the conversion to pixel value correctly identified our reference stars. Then we determined their corresponding instrumental magnitudes.

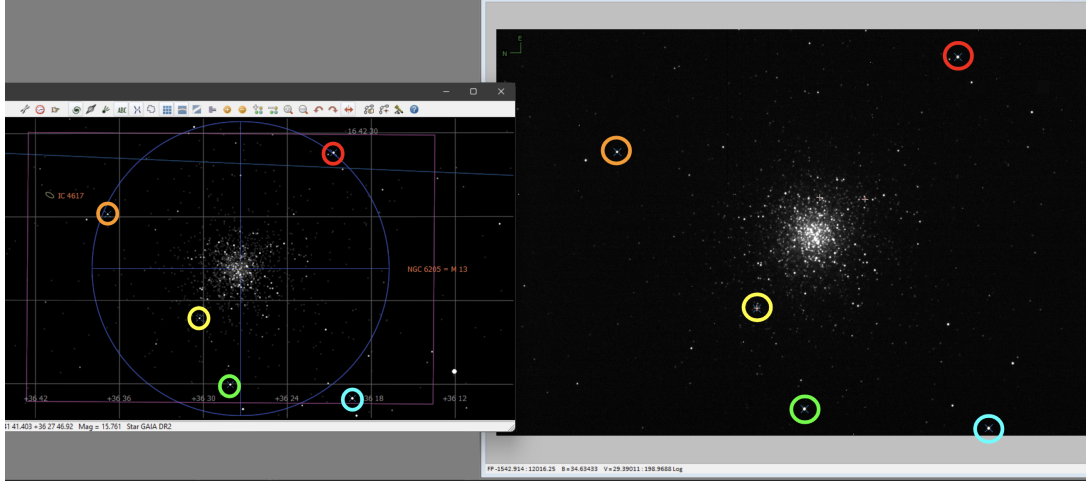


Figure 18: Matching Star Atlas database sources (left) with our chosen reference stars in our image (right) of M13. Matches are signified by the same color.

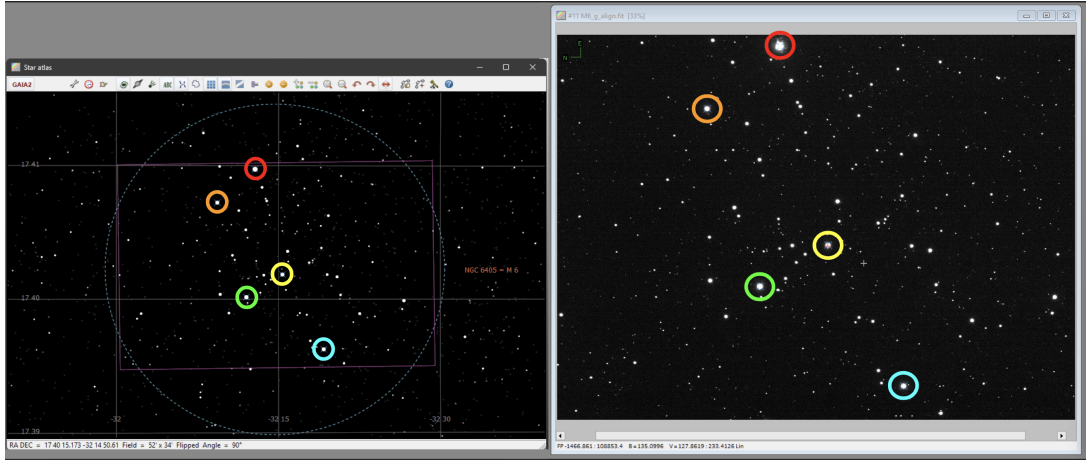


Figure 19: Matching Star Atlas database sources (left) with our chosen reference stars in our image (right) of M6. Matches are signified by the same color.

Now that we had the five instrumental magnitudes and their corresponding apparent magnitudes for each cluster, we could find ZP. We decided to use a linear fit of these data and set the slope to one to match equation 3. The y-intercept of this linear fit would be our ZP. By setting the slope to one, the calculation of the y-intercept is reduced to the average difference between absolute and instrumental magnitude, but a linear fit allows for a visual representation of this calculation. Shown in figures 20 and 21 are the linear fits in the R band for M13 and M6. The ZP we calculated is noted in the corner.

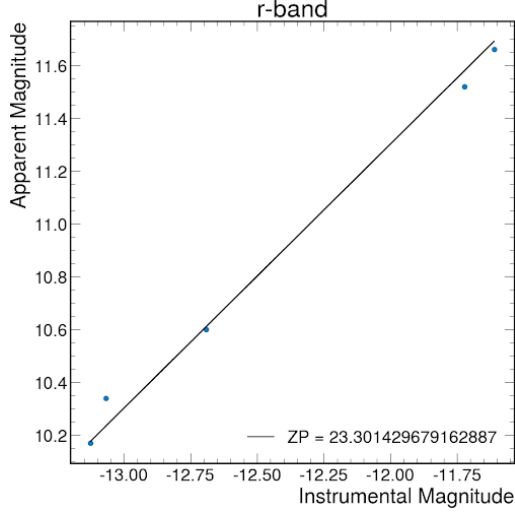


Figure 20: Plot depicting apparent magnitude vs instrumental R magnitude of our chosen reference stars in M13. A line of best fit restricted to a slope of 1 is shown and its y-intercept is noted.

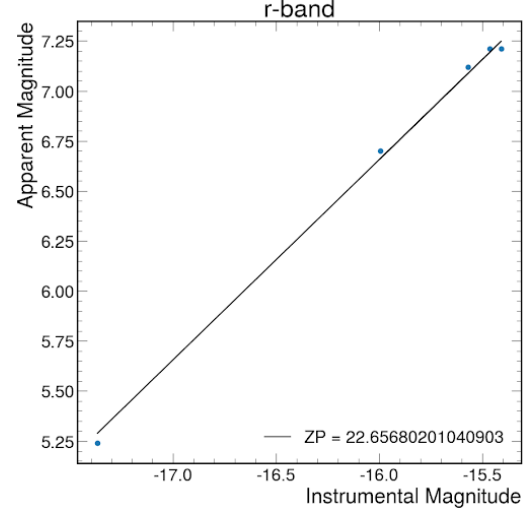


Figure 21: Plot depicting apparent magnitude vs instrumental R magnitude of our chosen reference stars in M6. A line of best fit restricted to a slope of 1 is shown and its y-intercept is noted.

We did this linear fit for the G and R band for both clusters. The ZPs for each filter and cluster are compiled in table 2 to the right. We then were able to convert all the instrumental magnitudes for all of our stars in each filter to their apparent magnitudes using the ZPs we calculated.

	$ZP_G$	$ZP_R$
M13	22.39	23.30
M6	23.20	22.65

Table 2: ZP values in each filter for M13 and M6.

As this process only involved adding a constant value to each instrumental magnitude, it did not change the shape or any trends on the diagrams. It was only a translation of the data points. This translation of the uncalibrated instrumental dataset to the calibrated apparent dataset is depicted in figures 24 and 25.

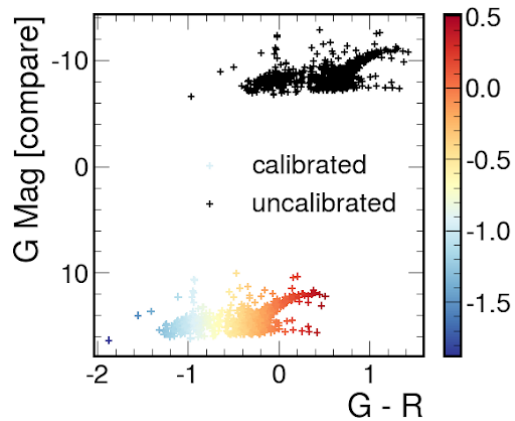


Figure 22: HR Diagram depicting our data pre-calibration (in black) and post-calibration (in color) of M13.

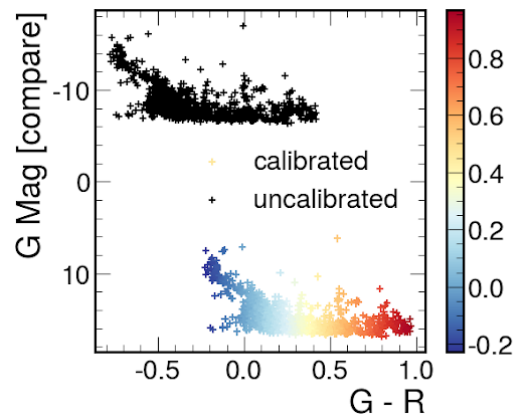


Figure 23: HR Diagram depicting our data pre-calibration (in black) and post-calibration (in color) of M6.

## F Final HR Diagrams

Finally, we had everything we needed to produce fully calibrated HR Diagrams of clusters M13 and M6. Depicted in figures 26 and 27, these diagrams plot G apparent magnitude against G-R color index. We added a color scale to enforce the idea that this difference in magnitude is related to the color of the stars, with lower differences corresponding to bluer stars.

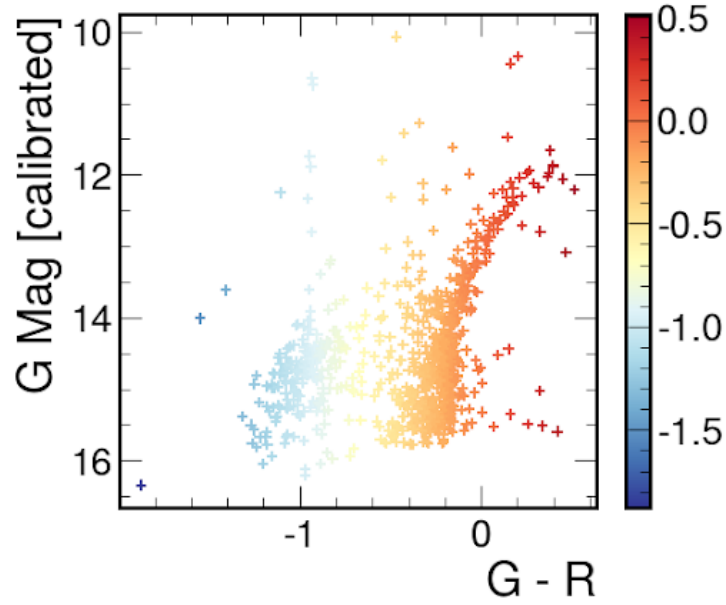


Figure 24: Final calibrated HR diagram of globular cluster M13.

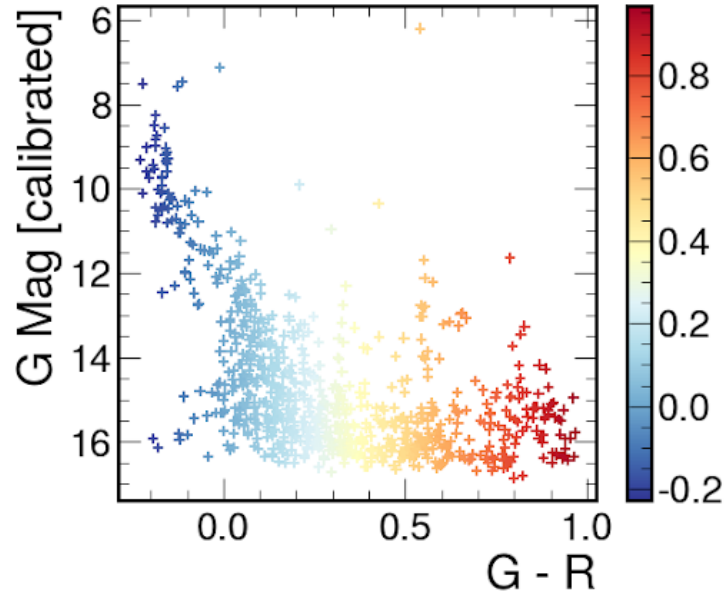


Figure 25: Final calibrated HR diagram of open cluster M6.

## V Final Analysis

Now that we have our completed HR diagrams, we can compare them to the HR diagrams we referenced earlier along with our IRG color images. We can use the trends on the plots to categorize the stars and tell us about clusters as a whole.

### A M13

Comparing this final HR diagram of M13 with the reference in figure 16, our shape and scale are very close to that of the reference. However, if we compare it to a typical HR diagram, like the one in figure 3, we do not see that main sequence diagonal that is characteristic of many HR diagrams. Instead, M13 is heavily populated by red giants and supergiants in the upper right, a few blue giants in the upper left, and some dwarfs and blue stragglers in the bottom.

As stars run out of hydrogen, they evolve off of the main sequence and begin fusing hydrogen as giants and supergiants. From our HR diagram, we can see that many of the stars are in this later stage of life. The turnoff point of this diagram is very red, suggesting that this is an older cluster. This aligns with other studies that have estimated this cluster to be almost over 11 billion years old.

Our HR diagram also looks like it well represents our color image of M13 in figure 6. It is mostly orange and red, with a little blue sprinkled in. The majority of the stars lie at around magnitude 15, with a few reaching magnitude 10 or 11. This almost aligns with the accepted 11.95 magnitude of V11, M13's brightest star. Our estimate is a little bright. However, this star is a variable star. Perhaps we caught it when it was a little brighter than normal, though it likely does not vary from nearly 12 to almost 10.

### B M6

When comparing this final HR diagram of M6 to the results of the photometric study in figure 17, we can also see that the trends and shapes are similar. In this case, we can directly compare the magnitude values. They used the same color index as we did since G-R is just a naming convention for the filters that represent B-V. The magnitudes we calculated tend to be slightly brighter than the magnitudes in the reference, with ours ranging from around magnitude 16 to 6 and the reference ranging from 14 to 8. The reference diagram also seems to have sigma clipped even more stars than we did as they plotted much fewer stars.

The diagram does have a more clear main sequence diagonal, and most of the stars lie on it. There are a few stars that veer off of the trend, such as the orange star at magnitude 6, which I can only assume is BM Scorpi, the orange giant that is known to be the brightest in the cluster.

This cluster does not have a turnoff point, suggesting that it is a very young cluster. There are many blue giants in M6, and most of the stars are in the relatively early stages of life. This is confirmed by other studies that have estimated that this cluster is only around 90 million years old, much younger than our solar system.

### C M13 & M6

Since we are confident in our HR diagrams of globular cluster M13 and open cluster M6 as they relate to previous studies and our CCD images, we can also compare between them and see what the comparison implies about globular and open clusters.

M13 is more populated by red giant and supergiant stars than M6, which contains more blue giant stars. Therefore, we can infer that open clusters are often more blue than globular clusters. We can support this inference by looking at our color images for each cluster.

Additionally, the HR diagram for M13 has a very clear and very red turnoff point while the diagram of M6 does not have one at all. As stated before, this suggests that M13 is very old while M6 is much younger. Therefore, we can hypothesize that globular clusters tend to be older than open clusters. These hypotheses align with the accepted knowledge of clusters discussed in section I.



## VI Error Analysis

### A Signal to Noise Ratio

All images will have some amount of noise. This noise is attributed to many different sources. Dark current is extraneous excitations of the camera, often due to temperature. Background noise due to light pollution scattered through the sky that is captured by the telescope. Readout noise involves leftover electrons from previous images that are recorded in subsequent CCD readouts.

Quantum efficiency is an image sensor's proficiency at converting incoming photons to electrons. Based on the spectral response curve depicted in figure 28, the kaf 6303 sensor has a maximum quantum efficiency of about 65% at red wavelengths and decreases at smaller wavelengths ( 52% for green and 40% for blue).

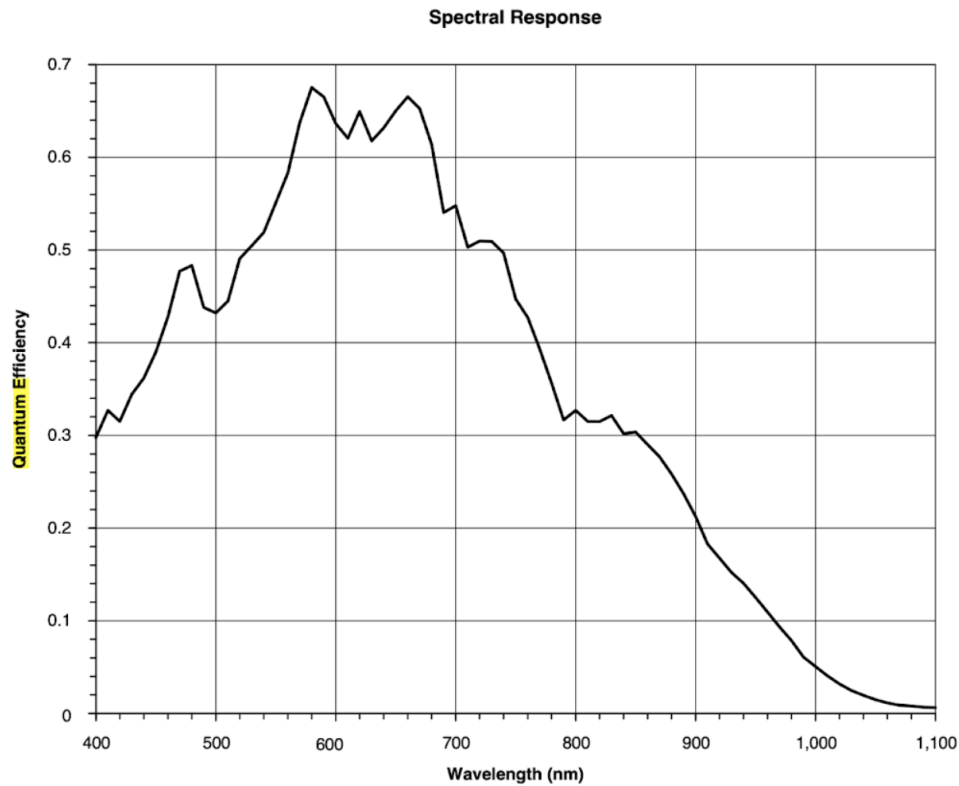


Figure 26: Spectral response of the kaf 6303 sensor plotted against wavelength. Credit: Onsemi [4]

As a result, the relative fluxes from each band may not only be from differences in the actual fluxes received by the sensor but will likely also include errors due to the different sensing capabilities at different wavelengths.

We can more clearly quantify all of these sources of noise using the equations and values listed in table 3.

Source of Error	Value/Equation
Readout noise	14.5 $e^-$
Dark current	0.03 at -100 C (estimated) $e^-/\text{pix-s}$
Background estimation	$\sigma_\beta = \sqrt{\pi r_{pho}^2 \mu_{bkgd}}$
Photon counts	$\sigma_S = \sqrt{S}$
Quantum Efficiency	$S = F\tau A\epsilon Q_e$

Table 3: Equations and values to quantify sources of noise.

These sources of error can be combined quadratically to find the signal to noise ratio (SNR) in each filter:

$$SNR = \frac{S}{N} = \frac{S}{\sqrt{\sigma_R^2 + \sigma_{DC}^2 + \sigma_\beta^2 + \sigma_S^2 + \sigma_{other}^2}} \quad (4)$$

The error in our magnitude calculations,  $\sigma_G$  and  $\sigma_R$ , can be estimated as  $\frac{1}{SNR}$ . Then, we can combine the error in G and R quadratically to find our G-R color index error:

$$\sigma_{G-R} = \sqrt{\sigma_G^2 + \sigma_R^2} \quad (5)$$

The SNR for each filter in each filter along with the error in our G-R color index that we calculated is compiled in table 4.

	M13	M6
SNR in G (dB)	76.152	87.440
SNR in R (dB)	81.078	82.402
$\sigma_{G-R}$	0.0433	0.0558

Table 4: The SNRs and errors we calculated for each filter and the color index in M13 and M6.

## B Linear Fit

When translating our instrumental magnitudes to apparent magnitudes, we did a linear fit to find the zero point constant ZP.

Exemplified by the residual plots shown in figures 27 and 28 for the R-band, the points did not lie exactly on our line of best fit. We used the formula for residual standard error:

$$RSE = \sqrt{\frac{\sum_{i=0}^n (y_i - \hat{y}_i)^2}{n - 2}} \quad (6)$$

where  $(y_i - \hat{y}_i)$  is the residual and  $n$  is the number of residuals. Our estimations of residual error are compiled in table 5.

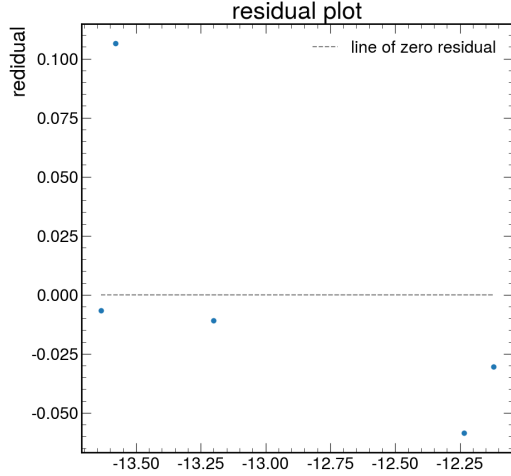


Figure 27: Residual plot of actual minus expected magnitude value in the R band of M13.

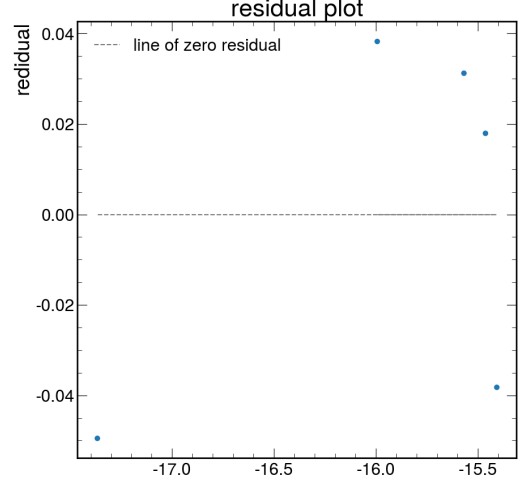


Figure 28: Residual plot of actual minus expected magnitude value in the R band of M13.

	M13	M6
RSE in G	0.5022	0.3564
RSE in R	0.0727	0.0846

Table 5: RSE in each filter for M13 and M6.

This demonstrates that there is some error in our estimate of ZR, more so in the green filter, and therefore, error in our conversion to apparent magnitude. The existence of this error reflects a systematic error in our measurements, since, theoretically, the instrumental magnitudes in a filter should all be related to their apparent magnitudes by the same exact number. This error can also come from our choice of reference stars, as they may have some variability that is not noted in the Star Atlas. These errors can be reduced by choosing more reference stars as inaccuracies due to measurement, poor choices in reference stars, and linear fit can be averaged out and minimized.

## VII Conclusion

In this investigation of star clusters, we went from CCD image outputs to fully calibrated Hertzsprung-Russell diagrams of globular cluster M13 and open cluster M6. We aligned the images to maintain image quality and used those images for two IRG color images and for all analyses down the line. Focusing on the G and R filters, we identified sources, masked messy data, and employed aperture photometry to convert the CCD output fluxes into instrumental magnitudes of stars. After making our first rough plot of our HR diagram, we implemented reference work and statistics to truncate our sources. Then we chose reference stars and did a linear fit to convert the instrumental magnitudes into the meaningful apparent magnitudes that we plotted in our final HR diagrams.

The diagram for M13 was full of red giants and supergiants. The diagram for M6 contained many blue giants. The turnoff point of M13 was deep in the red, suggesting that it is very old, and M6's clear main sequence diagonal implies that the cluster is much younger. These trends and shapes of our diagrams verified our previous understanding that globular clusters are redder and older while open clusters tend to be bluer and newer.

If we were to go through this process again, my first change would be to take images of M13 with shorter exposure times. This would hopefully make the image less oversaturated and help

resolve some of the congested center. Additionally, I would like to use more reference stars. This would hopefully decrease some of the linear fit error, making our absolute magnitude calculations more accurate.

For future study, I would enjoy looking into the cluster's proper motion to remove even more stars that could not be a part of the cluster. I think it would be the most helpful in M6 as there seem to be many more stars in the diagram than are actually believed to be in the cluster.

The study of star clusters has revealed some of the most important findings about stellar evolution in the past century. Studying open and globular clusters gives astronomers an opportunity to dissect the lifestyles of stars from thousands of light years away. HR diagrams, like the two we created, help solidify our understanding of these topics and allow us to use the tools to which we have access for astronomical discovery.

## References

- [1] Donatiello, Giuseppe. “Butterfly Cluster.” *Messier 6 - The Butterfly Cluster*, 2020, <https://www.flickr.com/photos/133259498@N05/50500635443/>. Accessed 10 June 2023.
- [2] “Globular Cluster.” *Hubble — ESA — NASA*, [esahubble.org/wordbank/globular-cluster/](http://esahubble.org/wordbank/globular-cluster/). Accessed 10 June 2023.
- [3] “Hertzsprung-Russell Diagram.” *Hertzsprung-Russell Diagram — COSMOS*, [astronomy.swin.edu.au/cosmos/h/hertzsprung-russell+diagram](http://astronomy.swin.edu.au/cosmos/h/hertzsprung-russell+diagram). Accessed 8 June 2023.
- [4] “KAF-6303.” Onsemi, <https://www.onsemi.com/pdf/datasheet/kaf-6303-d.pdf>.
- [5] Leach, Sid, and Adam Block. “Messier 13.” *M13 Hercules Star Cluster*, 17 Apr. 2008, [sidleach.com/m13.htm](http://sidleach.com/m13.htm). Accessed 8 June 2023.
- [6] “Magnitude and Color.” *Las Cumbres Observatory*, [lco.global/spacebook/distance/magnitude-and-color/](http://lco.global/spacebook/distance/magnitude-and-color/). Accessed 10 June 2023.
- [7] “Messier 6: Butterfly Cluster.” *Messier Objects*, 5 June 2023, [www.messier-objects.com/messier-6-butterfly-cluster/](http://www.messier-objects.com/messier-6-butterfly-cluster/).
- [8] “Messier 13: Hercules Globular Cluster.” *Messier Objects*, 1 Mar. 2022, [www.messier-objects.com/messier-13-hercules-globular-cluster/](http://www.messier-objects.com/messier-13-hercules-globular-cluster/).
- [9] “Open Cluster.” *Hubble — ESA — NASA*, [esahubble.org/wordbank/open-cluster/](http://esahubble.org/wordbank/open-cluster/). Accessed 10 June 2023.
- [10] Vanderbei, Bob. “Hertzsprung-Russell Diagram for M13.” *Hertzsprung-Russell Diagrams for Globular and Open Clusters*, <https://vanderbei.princeton.edu/images/NJP/HRdiag.html>. Accessed 11 June 2023.
- [11] Vleeming, G. “A photometric study of the open cluster M6 (NGC 6405).” *Astronomy and Astrophysics Supplement Series* 16 (1974): 331-342.

# Appendices

## A1 Code

All of the code used for this project is in our GitHub page organized by star cluster  
<https://github.com/Klinjin/134L/tree/main>

## A2 Visibility Calculator

Through LCO, we inputted the coordinates of M13 and M6 to make sure that they were visible this time of year. The following images are the outputs of this calculator, confirming that these targets were able to be observed

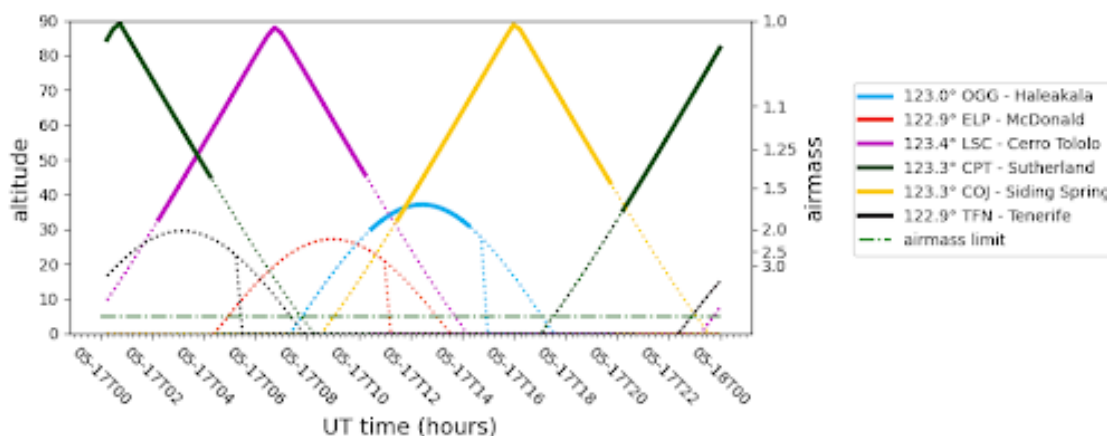


Figure 29: LCO visibility calculator output. Plot of altitude vs UTC time on a given day of M13.

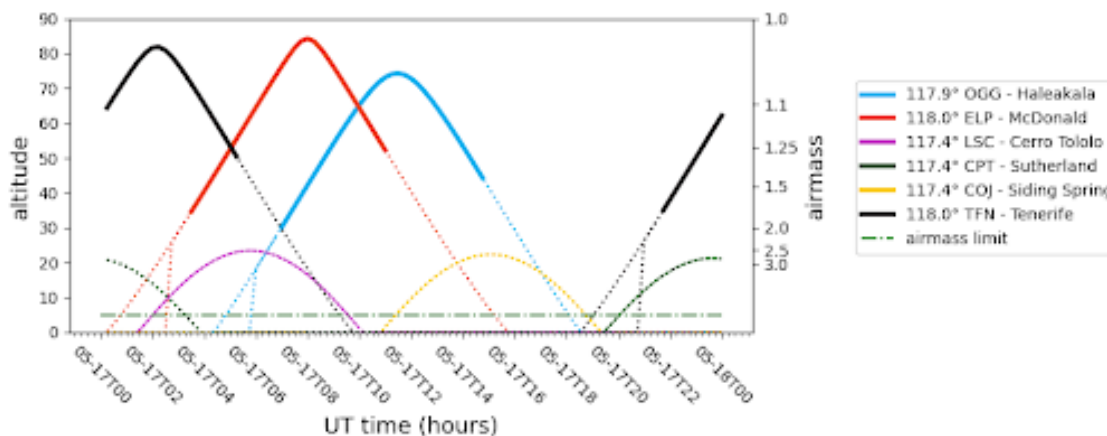


Figure 30: LCO visibility calculator output. Plot of altitude vs UTC time on a given day of M6.

## A4 Why we chose G and R

When we first began, we planned to use the U magnitude in our HR diagrams, as U-G is a common color index. After receiving our images, we quickly realized there was something wrong with the U band image. The images were entirely noise, so we decided to reassess and go with G and R.



### DAO Starfinder

We used DAO Starfinder for our first attempt at source identification. Even after tweaking a few parameters, the function was doing an almost random source extraction in the center of M13 and missing obvious stars in both clusters. This motivated us to find and use SEP Source extractor. The following images are the underwhelming sources found using DAO Starfinder.

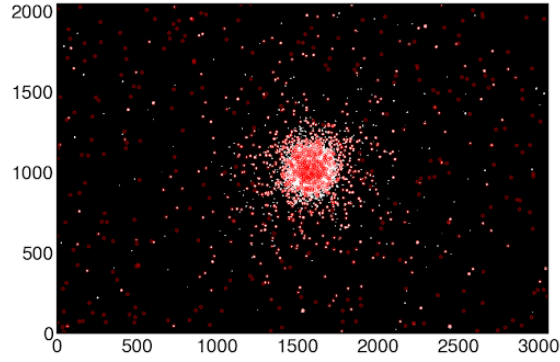


Figure 31: Sources found in M13 using DAO Starfinder

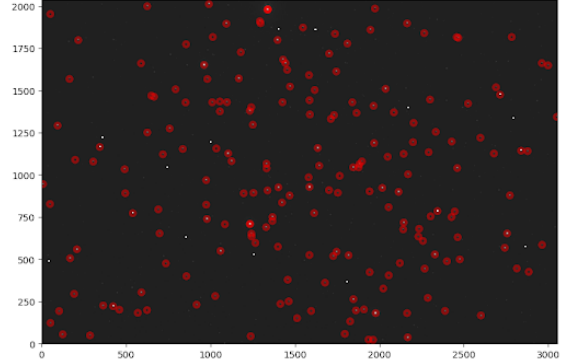


Figure 32: Sources found in M6 using DAO Starfinder.